A three-dimensional sound intensity measurement system for sound source identification and sound power determination by ln models[a)]

Shiho Nagata, Kenji Furihata,[b)] and Tomohiro Wada
Department of Electrical and Electronic Engineering, Faculty of Engineering, Shinshu University, 4-17-1 Wakasato, Nagano, 380-8533 Japan

David K. Asano
Department of Information Engineering, Faculty of Engineering, Shinshu University, 4-17-1 Wakasato, Nagano, 380-8533 Japan

Takesaburo Yanagisawa[c)]
Faculty of Engineering, Shinshu University, 4-17-1 Wakasato, Nagano, 380-8533 Japan

(Received 21 December 2004; revised 26 September 2005; accepted 27 September 2005)

This paper describes a full vector intensity probe which advances the field of sound intensity and sound source direction estimation using six matched rotating and variable directional microphones. The probe has three pairs of microphones at an equal spacing of 30 mm that are set up in each of the x, y, and z directions and share the same observation point. The calibration method using the rotating microphone system is effective to correct position errors in the y- and z-axes microphone pairs. Sound intensity measurements using the variable directional microphone method can locate with accuracy a sound source, i.e., the structure parts radiating most acoustic energy. The system can find the maximum sound intensity level and beamwidth of the major lobe, and the peak sound intensity levels of the minor lobes. Therefore, a procedure for sound power determination based on minimum measurement data is theoretically and experimentally discussed. Consequently, it is possible to reconstruct only parts of the system emitting the most noise and measure efficiently the sound power level. © *2005 Acoustical Society of America.* [DOI: 10.1121/1.2126929]

PACS number(s): 43.58.Fm, 43.55.Nd [AJZ] Pages: 3691–3705

I. INTRODUCTION

Sound intensity is a measure of the flow of energy passing through a unit area per unit time and is measured in W/m^2.[1] It is well known that the two-microphone method is very useful to determine the sound intensity vector in a sound field. A commonly used intensity probe consists of two closely spaced identical microphones, which are placed face to face.[2,3] However, there are three problems with this probe: (1) if there exists an intrinsic phase mismatch between microphones and/or channels, a so-called phase mismatch appears and the measurement error increases as the frequency decreases, (2) in the conventional technique based on deriving the particle velocity from the sound pressure gradient, if the two-microphone axis is not directed correctly toward the sound source, further errors result, and (3) from the probe's directional characteristics, this method is unable to separate the vectors precisely.

To solve problem (1), even a very small deviation between the phase responses of the two microphones, i.e., phase mismatch, has an adverse effect on the measurement accuracy with this technique,[4,5] so much effort has been spent on improving the transducers,[6] and on developing measurement procedures that ensure that the influence of the remaining phase mismatch is within acceptable limits.[7,8] One method of correcting such phase errors makes use of a switching technique that essentially performs measurements twice, the second time with the microphones interchanged.[9] Others methods make use of an initial calibration measurement where the two microphones are subjected to the same sound pressure, as in a small cavity.[10] Once the ratio for residual intensity to sound pressure used in determining the residual intensity has been determined, errors due to phase mismatch in subsequent intensity measurements can be corrected, provided that the mean square pressure is determined concurrently with the intensity.[11] In our proposed rotating microphone method,[12] which solves problems (1) and (2), the microphones are rotated around the measuring point in certain planes, and the data are processed numerically with use of periodic functions of the angles of rotation.

Some microphones allow us to vary the directional characteristics by selecting omnidirectional, cardioid, subcardioid, supercardioid, bidirectional, or shotgun patterns. In our variable directional microphone method,[13] which solves problem (3), the sound pressure spectrum of the microphone

[a)]Portions of this work were presented in "Three-dimensional sound intensity vector using a variable directional microphone system for identifying effective center of sound sources directly," Proceedings of Inter-Noise 2003, The 32nd International Congress and Exposition on Noise Control Engineering, Jeju, Korea, August 2003(N238), and "Fundamental study of the number of discrete measurement points on the sound power level using sound intensity method, " The 32nd International Congress and Exposition on Noise Control Engineering, Jeju, Korea, August 2003(N786).

[b)]Electronic-mail: kennfur@gipwc.shinshu-u.ac.jp

[c)]Professor Emeritus.

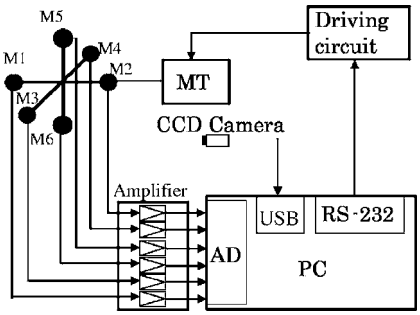

FIG. 1. Block diagram of our three-dimensional sound intensity measurement system.

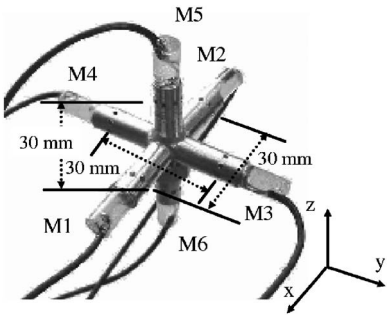

FIG. 2. Photo of our handmade three-dimensional sound intensity probe.

itself and the sound pressure gradient of the microphone pair are measured, the spectral amplitudes of both are compared, and only the sound incident from the desired direction is selected.

ISO 9614 governs sound power determination based on sound intensity. It is divided into two parts, one which makes use of point measurements (ISO 9614-1),[8] and one which makes use of swept or scanned measurements (ISO 9614-2).[14] The intention underlying the approach adopted in the ISO standard for sound power determination is to ensure that errors due to phase mismatch are within acceptable limits when some requirement is met, and to indicate actions to be taken in order to improve the situation when this is not the case. The switching technique and the rotating microphone method give in principle nearly perfect compensation for phase errors, but repeating the entire measurement is rather inconvenient. The calibration technique has never come into general use either, because of improvements in the available microphones, and partly because it seems to be surprisingly difficult to generate exactly the same sound pressure on the two microphones even in a very small coupler.[15]

The purpose of this paper is to discuss and demonstrate a three-dimensional sound intensity measurement system using six matched rotating and variable directional microphones in a symmetrical arrangement.[16] This system can measure the maximum sound intensity level and beamwidth of the major lobe, and the peak sound intensity levels of the minor lobes without the error sources of problems (1), (2), and (3). We also describe a sound power determination method based on minimum measurement data that seems to be surprisingly effective.

II. EQUIPMENT AND OPERATION PRINCIPLES

The following describes the operating principles of the proposed system. Figure 1 shows the block diagram of this system. It consists of a rotating intensity probe which has six microphones (M1–M6). The microphone outputs are amplified with six preamplifiers (gain: 60 dB) and the data are gathered using an eight-channel AD converter (Interface, PCI-3120, AD12P8D-79) and a personal computer (PC). MT is a stepping motor with a driving circuit, which is connected to the PC via an RS-232 interface. Sound intensity measurements offer several ways to locate and identify parts of devices and machines radiating the most acoustic energy. To identify visually each sound source, the proposed system is equipped with a small CCD (charge-coupled device) camera connected via a USB (universal serial bus) port.

A. Design of three-dimensional sound intensity probe

Figure 2 shows a photo of our handmade three-dimensional sound intensity probe. The probe has three pairs of microphones that are set up in each of the x, y, and z directions and share the same observation point. The microphones placed face to face in each pair are 30 mm apart. Each microphone is an electret condenser microphone (Star, MAA-06A-P, 6 mm in diameter). The frequency responses of these microphones are almost the same, and their sensitivity is about −43.0 dB(0 dB=1 V/Pa) from 100 Hz to 10 kHz.

LMS International SYSNOISE is effective for estimating the sound field around the probe structure. Figure 3 shows the diffraction effect in the sound field of our probe. From this figure, we see that the effect is less than 0.5 dB from 100 Hz to 2 kHz.

Thompson and Tree[17] considered the errors due to developmental finite difference approximations in the two-microphone acoustic intensity measurement technique. The best procedure would be to select measurement parameters based on the quadrupole nondimensional analysis as a worst-case design. Therefore, the parameter limits $0.1 \leqslant k\Delta r \leqslant 1.3$ and $0 \leqslant \Delta r/r \leqslant 0.5$ (k is the acoustic wave number, Δr is the microphone separation, and r is the distance between a source and the measurement point) would be useful guidelines for maximum inaccuracy for ±1.5 dB. Therefore, a microphone separation of 30 mm can cover frequencies from 182 Hz to 2.37 kHz.

For a sound field generated by a simple source, it can be shown that $|I_r|/|I_\infty| \approx \sin(k\Delta r)/k\Delta r$ in the far field, where I_∞

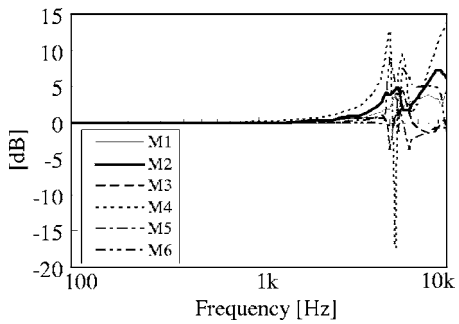

FIG. 3. Diffraction effect in the sound field of our probe predicted with LMS SYSNOISE.

indicates the magnitude of the far-field intensity. The magnitude of the far-field intensity is measured using the conventional mean-squared-pressure measurement, i.e., $|I_\infty| = \overline{p^2}/\rho c$, where $\overline{p^2}$ is the mean squared pressure, ρ is the air density, c is the speed of sound, and I_r is the radial intensity, which is measured at the same location in the direction pointing from the source to the measurement location. This expression shows that for $k\Delta r \leqslant 1$ ($k\Delta r = 1$ corresponds to 1.8 kHz, since $\Delta r = 30$ mm in this case) the deviation of $|I_r|$ from $|I_\infty|$ is less than 1 dB.[9]

B. Calibration of the rotating microphone system

The calculation of the sound intensity in the two-microphone method is very sensitive to any phase mismatch between the two microphones. However, in general, there are phase mismatches between each pair of microphones in our system. Therefore, a sound-pressure phase-difference calibrator is necessary to make the probes easy to use. Because our initial acoustic intensity measurement searches for the maximum sound intensity level of the major lobe, its beamwidth, and the peak sound intensity levels of the minor lobes, our three-dimensional sound intensity measurement system makes use of an initial calibration measurement where the three pairs of microphones are subjected to the same sound pressure.

To meet the most stringent requirements for measurement accuracy, calibration of the sound intensity probe and sound intensity level was done in our faculty's anechoic room ($3 \times 4 \times 5 = 60$ m^3). The loudspeaker used as the simple source was a dynamic type with a diameter of 16 cm. The back was sealed with clay. A sampling frequency of 32 kHz was used for the sound intensity measurements which gives us a Nyquist frequency of 16 kHz. Depending on the measurement accuracy,[18] the FFT sizes of 1024, 2048, and 4096 were used yielding 512, 1024, and 2048 frequency data points, respectively. Therefore, the complex transfer functions were measured using the above-noted FFT sizes.

Consider one pair of microphones. A sound wave front that reaches microphone M1 will reach microphone M2 after a certain time delay. The difference in time is used to calculate the sound intensity component on the microphone axis and to judge the direction of the sound as either backward or forward. Assuming the sound pressure at M1 is $p_1(t)$ and that at M2 is $p_2(t)$, then the average value of the sound pressure $p(t)$ and the particle velocity $v(t)$ is

$$p(t) = \frac{p_1(t) + p_2(t)}{2}, \tag{1}$$

$$v(t) = -\frac{1}{\rho} \int \frac{\{p_2(t) - p_1(t)\}}{\Delta r} dt, \tag{2}$$

where Δr is the distance between the two microphones and ρ is the air density. The sound intensity can be determined by multiplying $p(t)$ by $v(t)$ and calculating the time average for this product.[19]

Figure 4 shows the configuration of a sound source and the microphone orientation (four microphones) in Cartesian coordinates. When we direct the x-axis probe toward the sound source, the sound intensity I is given by[12]

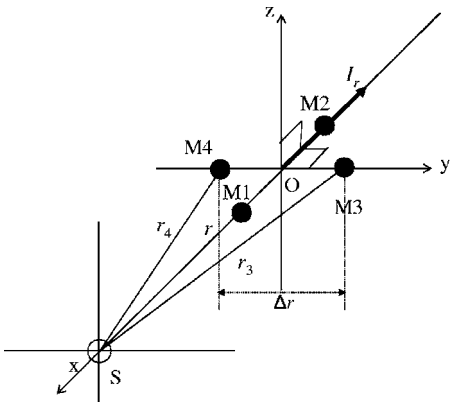

FIG. 4. Configuration of a sound source S and four microphones in Cartesian coordinates. O is the observation point (the center of our probe), M1, M2, M3, and M4 are the locations of the measuring microphones, r is the distance from O to S, r_3 is the distance from M3 to S, r_4 is the distance from M4 to S, and Δr denotes the microphone separation.

$$I = I_x = \frac{\overline{p^2}}{\rho c}\left(1 + \frac{\phi_{12}}{k\Delta r}\right), \tag{3}$$

where ρc is the specific acoustic impedance, k is the wave number, and ϕ_{12} is the phase mismatch between M1 and M2.

First, sound intensity levels were measured using this system (I_x) and an intensity level measuring system (I_r) by the cross-spectral method (RION Co., SA-74),[2,3] consisting of an intensity microphone (RION Co., SI-21, which has a maximum intrinsic phase mismatch of 0.25° at 150 Hz), a pistonphone (NC-72), and a FFT analyzer (SA-74). The two intensity probes were set 4 m away from the front of the loudspeaker.

From the results, the bias error $\phi_{12}/k\Delta r$ is given by

$$\frac{\phi_{12}}{k\Delta r} = \left|\frac{I_x}{I_r}\right| - 1. \tag{4}$$

Therefore, it can be seen that once the bias error $\phi_{12}/k\Delta r$ has been determined, errors due to phase mismatch in subsequent intensity measurements can be corrected. Figure 5 shows the bias error $\phi_{12}/k\Delta r$ (solid line) as a function of frequency (FFT size: 1024). From this figure, we see that

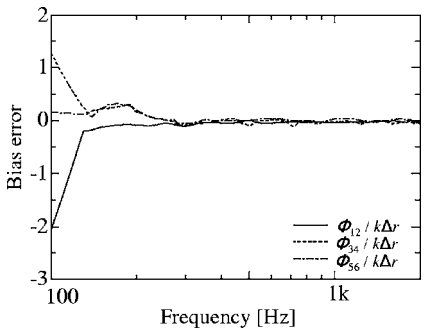

FIG. 5. Bias errors $\phi_{12}/k\Delta r$, $\phi_{34}/k\Delta r$, and $\phi_{56}/k\Delta r$ as a function of frequency.

the bias error is −2.1 at 100 Hz, and ±0.1 or less from 200 Hz to 2 kHz.

Second, the sound intensity I_y with a bias error due to the phase error ϕ_{34} between microphones M3 and M4 can be written as

$$I_y = \frac{\overline{p^2}}{\rho c} \cdot \frac{\phi_{34}}{k\Delta r}. \tag{5}$$

Similarly, the sound intensity I_z with a bias error due to the phase error ϕ_{56} between microphones M5 and M6 can be written as

$$I_z = \frac{\overline{p^2}}{\rho c} \cdot \frac{\phi_{56}}{k\Delta r}. \tag{6}$$

Consequently, if the y-axis and z-axis probes were to be rotated around the x-axis probe in the y-z plane, the sound intensity components given by Eqs. (5) and (6) would be obtained as functions of the rotation angle $\theta = 2\pi(i-1)/N$.[12] These would be periodic functions of the angle of rotation, containing the bias errors.

Accordingly, to cancel the bias errors from Eqs. (5) and (6), one can multiply them by the periodic function $e^{j\theta}$ and then integrate the results over the period of rotation, resulting in

$$\frac{1}{\pi}\int_0^{2\pi} I_y e^{j\theta} d\theta = \lim_{N\to\infty} \sum_{i=1}^{N} \frac{2}{N} I_y \exp\left(j\frac{2\pi}{N}(i-1)\right)$$

$$= \sum_{i=1}^{3} \frac{2}{3} I_y \exp\left(j\frac{2\pi}{3}(i-1)\right) = 0, \tag{7}$$

$$\frac{1}{\pi}\int_0^{2\pi} I_z e^{j\theta} d\theta = \lim_{N\to\infty} \sum_{i=1}^{N} \frac{2}{N} I_z \exp\left(j\frac{2\pi}{N}(i-1)\right)$$

$$= \sum_{i=1}^{3} \frac{2}{3} I_z \exp\left(j\frac{2\pi}{3}(i-1)\right) = 0. \tag{8}$$

From Eqs. (7) and (8), it is clear that when the components along each axis are zero, the x-axis probe is correctly directed toward the sound source, and the sound intensity I_r is given by Eq. (3). In this way, when our probe was set with the components along each axis equal to zero, the bias errors of Eqs. (5) and (6) can be determined. Figure 5 shows the bias errors of $\phi_{34}/k\Delta r$ (dashed line) and $\phi_{56}/k\Delta r$ (dash-dot line). From this figure, it can be seen that the bias errors of the sound intensities I_y and I_z have been determined, too. Therefore, the bias errors of our probe due to phase mismatches in subsequent intensity measurements can be corrected.

C. Variable directional microphone method (Ref. 13)

A complicated structure may radiate sound from several sources and absorb sound in other places. To evaluate the effectiveness of noise reduction methods we need to know how much noise is being radiated by the individual components of machines. The directivity characteristics for the sound intensity analysis system looks (two-dimensionally) like a figure-eight pattern, known as a cosine characteristic. This is due to the probe and the calculations done by the analyzer. For sound incident at an arbitrary angle α to an axis, the intensity component along the axis will be reduced by a factor of $\cos\alpha$. For sound incident at 90° to an axis, there is no component along the axis, as there will be no difference in the pressure signals. Hence there will be zero particle velocity and zero intensity. The full vector is made up of three mutually perpendicular components (at 90° to each other); one for each coordinate direction. Therefore, there is a change in direction for only a small change in the incident angle. The position of the measurement probe where the sound intensity direction alternates rapidly between positive- and negative-going intensities defines the point where the sound source must be incident on the probe at 90° to its axis. In this way, a technique using a variable directional microphone system that is able to separate a sound intensity vector is proposed.

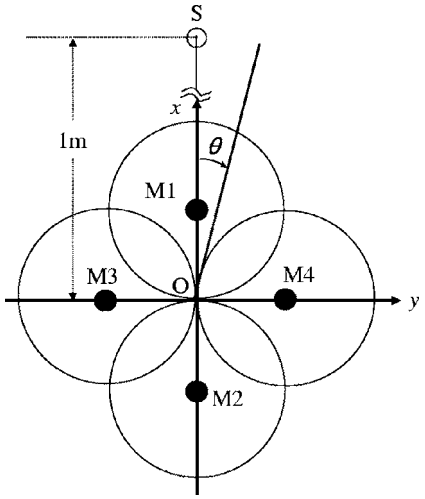

FIG. 6. Relationship between the directional separation angle θ and the microphone orientation. S is a sound source, r is the distance from O to S, and M1, M2, M3, and M4 are the locations of the measuring microphones.

Figure 6 shows the relationship between the separation angle and the microphone orientation (four microphones: M1, M2, M3, and M4) in the two-dimensional x-y sound field. In this figure, a directional separation angle θ is set on the x-y plane. When the intrinsic phase mismatches between each pair of microphones are zero, the sound intensity components I_x and I_y in the θ direction are given by

$$I_x = \frac{\overline{p^2}}{\rho c}\cos\theta, \tag{9}$$

$$I_y = \frac{\overline{p^2}}{\rho c}\cos(\theta - 90°). \tag{10}$$

Therefore, the relationship of the sound intensity level difference LD between I_x and I_y to the directional separation angle θ can be written as

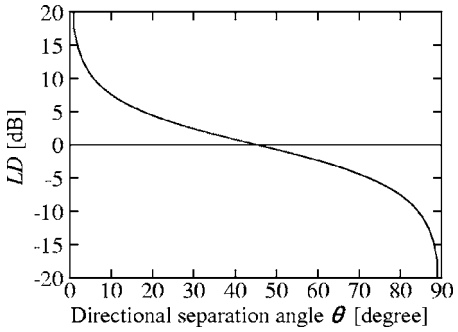

FIG. 7. Relationship between the level difference LD and the directional separation angle θ.

$$\mathrm{LD} = 10\log_{10}\left|\frac{I_x}{I_y}\right| = 10\log_{10}\left|\frac{\cos\theta}{\cos(\theta-90^\circ)}\right| (\mathrm{dB}). \quad (11)$$

Figure 7 shows the relationship between the level difference LD and the directional separation angle θ. From this figure, it can be found that when θ=5.7°, 10°, and 15°, LD =10.0, 7.5, and 5.7 dB, respectively.

1. Variation of the directional separation angle and its effectiveness

First, verification of the directional separation angle of the microphone system by Eq. (11) was carried out. In the experiment, a speaker S (a distance r=1 m from the sound source to the center of our probe) in the direction θ=0° was driven by a 1 kHz pure tone in our faculty's anechoic room. The sound intensity was measured while the probe was rotated in 1.8° steps at directional separation angles θ of 5.4°, 16.2°, and 30.6° (LD=10.24, 5.37, and 2.28 dB, respectively).

The measured results for the directional separation angles shown in Fig. 8 are normalized by the intensity level at the direction of the sound source (θ=0°). From Figs. 8, we see that the measured results, indicated by closed triangles, and the theoretical directional separation angles (θ =5.4°, 16.2°, and 30.6°), indicated by the solid lines, agree well, because the bias errors are zero. Therefore, it can be verified experimentally that the directional separation angle θ can be set arbitrarily.

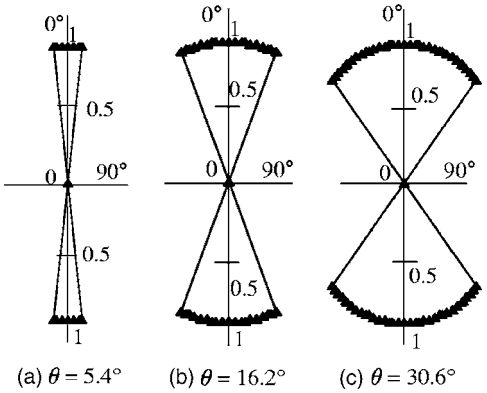

FIG. 8. Measured separation angle using our variable directional microphone method when the sound source was driven by a 1 kHz sine wave. Solid lines: theoretical value, and closed triangles: measured value.

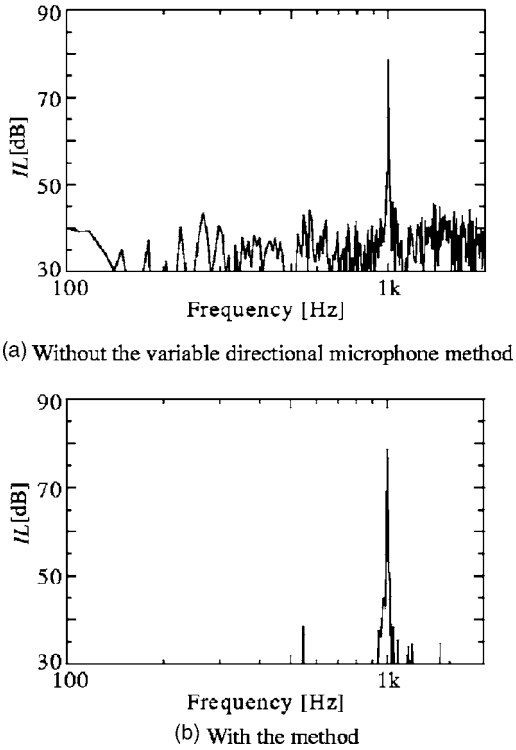

FIG. 9. Comparison of the measured results (a) without and (b) with the variable directional microphone method when the directional separation angle θ=5.7°, S_1 (1 kHz sine wave, and θ_1=0°), and S_2 (band noise from 128 Hz to 2 kHz, and θ_2=30°).

Second, the experiment on the signal from the desired sound source direction was carried out by simultaneously driving speaker $S_1(\theta_1=0^\circ)$ with a 1 kHz pure tone and speaker $S_2(\theta_2=30^\circ)$ with passband noise (128 Hz to 2 kHz) in our faculty's anechoic room. To separate the signals from S_1 and S_2, the directional separation angle θ was set 5.4°.

Figure 9(a) shows the sound intensity measured without the variable directional microphone method and Fig. 9(b) with the method. From Fig. 9(b), we see that the desired sound intensity spectrum (1 kHz) was separated from the sound intensity spectrum due to passband noise. Consequently, it can be said that the proposed method can separate sound intensity vectors of sound sources with different spectra.

2. Sound source identification

Figure 10 shows a block diagram of our equipment used to identify sound sources in a vacuum cleaner. The vacuum cleaner was rotated by a handmade turntable (0.04° / pulse) with a pulse motor and pulse motor control system. The distribution of each sound source was measured by our system at a distance of 10 cm from the vacuum cleaner at heights of 10, 20, 30, and 40 cm from the mesh floor in our faculty's anechoic room. The directional separation angle θ was set to 16.2°.

Contour and three-dimensional plots give a more detailed picture of the sound field generated by a sound source. Figure 11 shows contour plots of several sound sources in

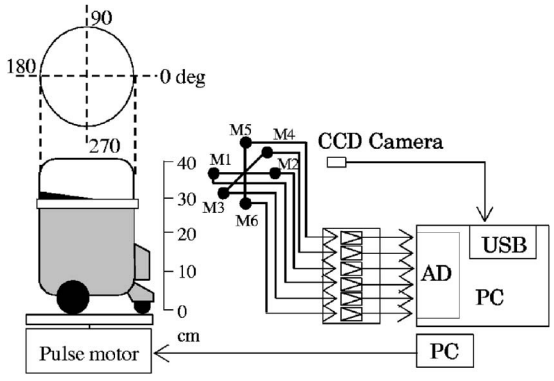

FIG. 10. Block diagram of the equipment used to identify the sound sources in a vacuum cleaner.

the vacuum cleaner at (a) 601 Hz and (b) 1828 Hz. From Fig. 11, it can be found that the sources and/or sinks can be identified with accuracy.

3. Source location—The null search method on the y-z plane

As a quick and easy test we can make use of the probe's directional characteristics. Sound incident at 85° to the axis will be recorded as positive-going intensity, whereas sound at 95° will give negative-going intensity. Therefore there is a change in direction for only a small change in angle. For example, Fig. 12 shows a three-dimensional intensity display of our sound intensity measuring system. Measurements (the sampling frequency; 32 kHz, FFT size; 1024 points) were

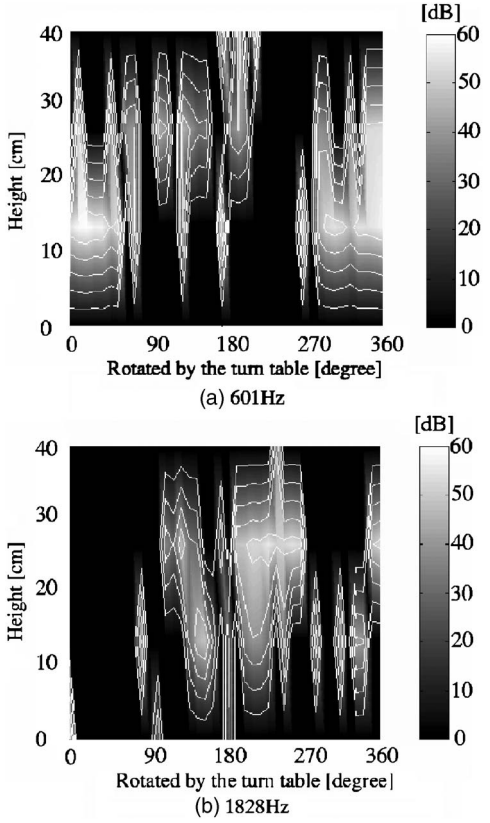

FIG. 11. Contour plots of the sound intensity distribution of the vacuum cleaner.

done every 0.113 s. While we watched the display, the probe was swept so that its axis followed a line parallel to the *y-z* plane on which the source was located. At some point, the direction suddenly changed as shown in the center figure $[\mathbf{I}_y(\mathrm{dB})]$ in Fig. 12. Here the sound must be incident on the *x*-axis probe at 90° to the *y* axis and thus identifies the source position. Figure 13 shows a picture taken by the CCD camera at the sound source identified visually as shown in Fig. 11.

Consequently, it can be said that this technique is effective to determine the location of sound sources and the amount of noise being radiated by the individual components of machines.

III. SOUND POWER DETERMINATION PROCEDURE

Requirements for sound power determination as part of a more general product noise measurements are becoming more and more widespread. One reason for this is the increasing amount of legislation regarding noise emissions. Sound intensity is a vector and is a measure of acoustic energy flow. It has a fundamental advantage in sound power determination since there is a direct connection between sound power and sound intensity. In theory, all that is required to measure the sound power of a source is to integrate the sound intensity over a surface totally enclosing the source based on Gauss's theorem.[20] Because of the vector nature of intensity, the effects of any noise sources external to the surface will cancel out. In practice, however, imperfections in the measuring equipment and measuring technique make the procedure rather complicated.

ISO 9614 governs sound power determination based on sound intensity. It is divided into two parts, one which makes use of point measurements (ISO 9614-1),[8] and one which makes use of swept or scanned measurements (ISO 9614-2).[14] Point measurements can be used for precision, engineering, and survey grade determination of sound power. The number of measurement points used in these methods tends to increase, i.e., the sound power level PWL can be calculated using the sound intensity method with the following:

$$\mathrm{IL}_i = 10 \log_{10} I_{ni}/I_0 \ (\mathrm{dB}), \quad I_{ni} = I_0 \cdot 10^{IL_i/10} \ (\mathrm{W/m^2}), \tag{12}$$

$$W \cong \sum_{i=1}^{N} I_{ni} \Delta S_i \ (\mathrm{W}), \tag{13}$$

$$\mathrm{PWL} = 10 \log_{10} W/W_0 \ (\mathrm{dB}), \tag{14}$$

where IL is the sound intensity level in dB, I_n is the normal sound intensity, $I_0 = 10^{-12}$ W/m^2, and $W_0 = 10^{-12}$ W.

ISO 9614-1 recommends starting with ten measurement positions. The number of measurement points N is determined from the nonuniformity field indicator F_4 using

$$F_4 = \frac{1}{\bar{I}_n} \sqrt{\frac{1}{N-1} \sum_{i=1}^{N} \left(I_{ni} - \bar{I}_n\right)^2}, \tag{15}$$

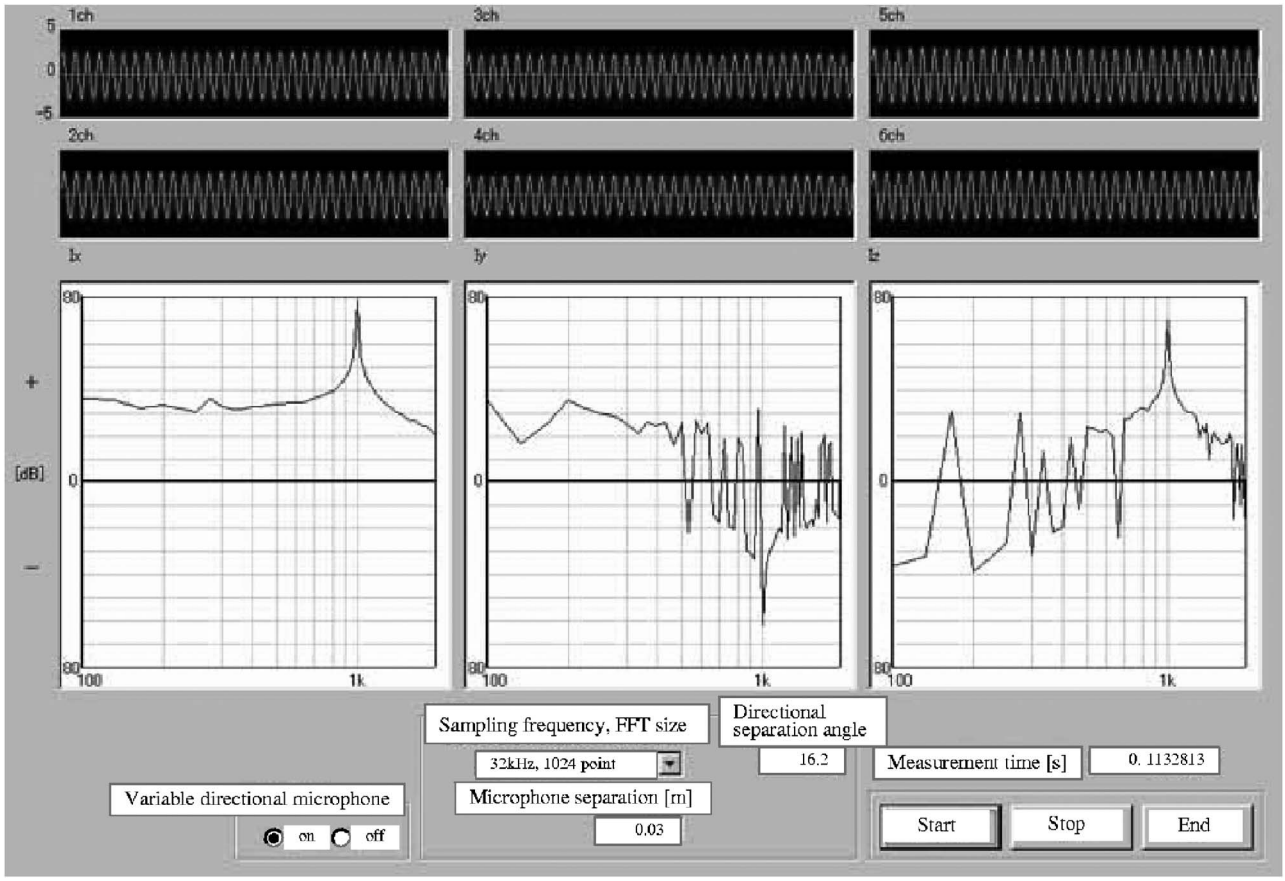

FIG. 12. An example of the three-dimensional intensity display of our sound intensity measuring system. Measurements (sampling frequency: 32 kHz, FFT size: 1024 points) were done every 0.113 s.

$$N > CF_4^2, \tag{16}$$

where $\bar{I}_n$ is the average normal sound intensity, and C is a constant depending on the required measurement accuracy. The values for C are: 11 when the 1/3 octave band center frequency is 100–160 Hz, 19 when the center frequency is 200–630 Hz; and 29 when the center frequency is 800 Hz to 5 kHz. ISO 9614-1 yields accuracy in the mid-frequency range (800–5000 Hz) of 1.0 dB for precision grade and 1.5 dB for engineering grade. From Eqs. (15) and (16), the number of measurement points is decided according to the variation in the sound intensity on the measurement surface. Therefore, many measurement points are required when the value of F_4 is large.

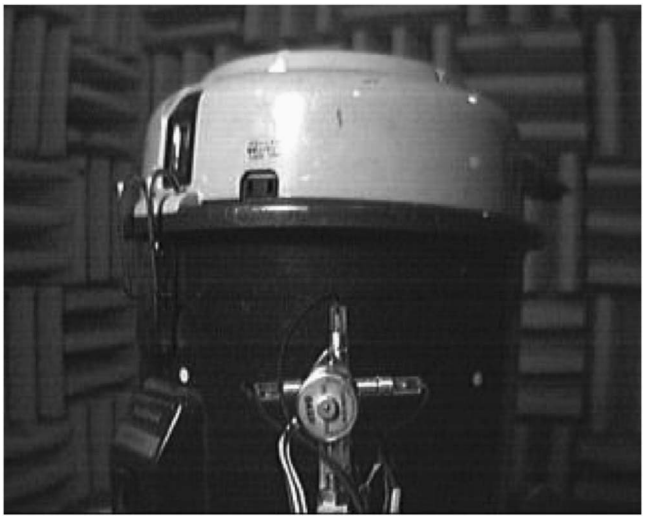

FIG. 13. Picture taken by the CCD camera at the position of the maximum sound intensity of the sound source.

A. Theory of sound power determination based on minimum measurement data

In general, sound waves produced by most sources have pronounced directional effects known as the directivity of the source. The number of measurement points is influenced by the directivity of the sources.

The sound power level of an omnidirectional sound source is given by

$$W = 4\pi r^2 I \ (\mathrm{W}),$$

$$\begin{aligned} \mathrm{PWL} &= \mathrm{IL} + 10\log_{10} 4\pi + 10\log_{10} r^2 \\ &= \mathrm{IL} + 10.99 + 20\log_{10} r \ (\mathrm{dB}), \end{aligned} \tag{17}$$

where r is the distance from the sound source to the measurement point. In this case, it is necessary to measure value of IL, which is the same in any direction.

The sound power level taking into account the directivity of the source is given by

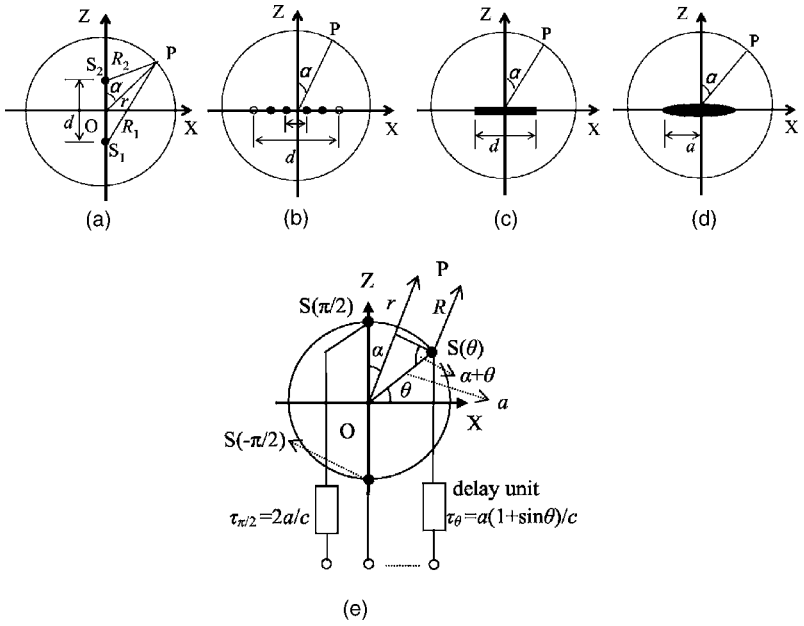

FIG. 14. Sound source location of each model: (a) a dipole source, (b) a model sound source with $n=2$ and 6 point sources of the same phase, (c) a line sound source, (d) a circular diaphragm, and (e) a circular array source with delay units.

$$\begin{aligned}\mathrm{PWL\_}D_i &= \mathrm{IL_{peak}} + 10\log_{10} 4\pi + 10\log_{10} r^2 + D_i \\ &= \mathrm{IL_{peak}} + 10.99 + 20\log_{10} r + D_i \ (\mathrm{dB}),\end{aligned} \tag{18}$$

where D_i is the directivity index.[21–23] The directivity index $D_i = 10\log_{10}(D_r)$ (dB) is simply the decibel expression for the directivity ratio D_r. In general, D_r is calculated from the directivity factor $D(\alpha)$ using

$$D_r = \frac{1}{4\pi}\int_0^{4\pi} D^2(\alpha)d\alpha. \tag{19}$$

When the directivity factor $D(\alpha)$ is symmetrical to a reference axis, Eq. (19) can be written as

$$D_r = \frac{1}{2}\int_0^{\pi} D^2(\alpha)\sin\alpha d\alpha. \tag{20}$$

Therefore, the sound power level can be calculated from the peak sound intensity level, the distance from the observation point to the source, and the directivity index.

This section discusses whether the directivity index can be theoretically calculated from the maximum directivity ratio, the beamwidth, and the surface area of minor lobes.

1. The directivity factor of model sound sources

This paragraph discusses the directivity factor of some model sound sources. Model sound sources are (a) a dipole source, (b) a model sound source with two or six point sources (two monopole sources of equal strength and same phase, and six monopole sources), (c) a line sound source, (d) a circular diaphragm, (e) a bidirectional sound source, (f) a cardioid sound source, (g) an end fired line source, and (h) a circular array source with delay units.

a. A dipole source (Refs. 24 and 25). A typical kind of source is a dipole source consisting of two monopole sources (S_1 and S_2) of equal strength but opposite phase and separated by a small distance compared with the sound wavelength as shown in Fig. 14(a). In this figure, d is the distance between two monopole sources, r is the distance from the origin O to P, α is the angle made by the line segment OP and the z axis, R_1 is the distance from the monopole source S_1 to P, and R_2 is the distance from the monopole source S_2 to P. The instantaneous value of the volume velocity of S_1 is $-\sqrt{2}\dot{U}e^{j\omega t}$, and the instantaneous value of the volume velocity S_2 is $\sqrt{2}\dot{U}e^{j\omega t}$, where $\dot{U}$ is the root mean square complex volume velocity.

The directivity factor is given by

$$D(\alpha) = \left|\sin\left(\frac{kd}{2}\cos\alpha\right)\right|, \tag{21}$$

where $k=\omega/c$ is the wave number and c is the speed of sound. The directivity has a rotational symmetry, and the characteristic changes with kd.

An expression for the theoretical sound intensity I is given by

$$I = \mathrm{Re}\left[\frac{1}{2}pv^*\right] = \frac{k^2\rho c|\dot{U}|^2}{(2\pi r)^2}\sin^2\left(\frac{kd}{2}\cos\alpha\right), \tag{22}$$

where v^* is the complex conjugate of the particle velocity, ρ is the air density. In this case, the theoretical sound power radiated is given by

$$\begin{aligned}W &= \int_s IdS = r^2\int_0^{\pi} I\sin\alpha d\alpha\int_0^{2\pi} d\beta = 2\pi r^2\int_0^{\pi} I\sin\alpha d\alpha \\ &= \frac{2|\dot{U}|^2\rho\omega^2}{4\pi c}\left(1-\frac{\sin kd}{kd}\right),\end{aligned} \tag{23}$$

where β is the directional angle from the x axis on the x-y plane.

b. A model sound source with n point sources (Ref. 21). The directivity factor is given by

$$D(\alpha) = \left| \frac{\sin nx}{n \sin x} \right|, \tag{24}$$

where n is the number of sound sources, and $x = (kd/2)\sin\alpha$.

Figure 14(b) shows a model sound source with two or six point sources in a line.

c. A line sound source (Ref. 21). Figure 14(c) shows a line sound source. The directivity factor is given by

$$D(\alpha) = \left| \frac{\sin x}{x} \right|, \tag{25}$$

where $x = (kd/2)\sin\alpha$.

d. A circular diaphragm (Refs. 21,23,25). The radiation pattern of sound intensity was calculated using the directivity factor of a circular diaphragm which was fitted into a rigid wall and vibrated like the piston. Figure 14(d) shows a circular diaphragm. The directivity factor is given by

$$D(\alpha) = \left| \frac{2J_1(ka \sin\alpha)}{ka \sin\alpha} \right|, \tag{26}$$

where J_1 is the Bessel function of the first kind of order one, and a is the radius of the circular diaphragm.

The radiation of sound is zero at certain angles from the axial direction of the source, and also has local maximi. The second local maximum, called the minor lobe, is usually much weaker than the first maximum (the major lobe) at a smaller angle. The beamwidth[23] is defined as the angle at which the sound intensity drops to one half of its value at the axial direction to the source.

e. A bidirectional sound source (Ref. 22). For a typical sound source, the bidirectional directivity factor is defined as

$$D(\alpha) = |\cos\alpha|. \tag{27}$$

Because the directivity can be made sharper by multiplying Eq. (27) by itself, a more general directivity factor is given by

$$D(\alpha) = |\cos^m \alpha|. \tag{28}$$

The values of m used are integers from 1 to 11.

f. A cardioid sound source (Ref. 22). For a typical sound source, the directivity factor of cardioid is defined as

$$D(\alpha) = |(1 + \cos\alpha)/2|. \tag{29}$$

Because the directivity can be made sharper by multiplying Eq. (29) by itself, a more general directivity factor is given by

$$D(\alpha) = |[(1 + \cos\alpha)/2]^m|. \tag{30}$$

The values of m used are 1/8, 1/7, 1/6, 1/5, 1/4, 1/3, 1/2, and integers from 1 to 11.

g. An end fired line source (Ref. 21). An end fired line source is one in which there is progressive phase delay between the elements arranged in a line. When the excitation time delay between the elements corresponds to the wave propagation time in space for this distance, the maximum directivity occurs in the direction corresponding to the line joining the elements. The directivity factor of this type of end fired line and of uniform strength is given by

$$D(\alpha) = \left| \sin\left[\frac{k}{2}(d - d\cos\alpha) \right] \Big/ \frac{k}{2}(d - d\cos\alpha) \right|, \tag{31}$$

where d is the length of the line.

h. A circular array source with delay units (Ref. 26). The direction and shape of the wave front produced by a circular array of sound sources may be altered by the introduction of a delay pattern in the excitation of the sources as shown in Fig. 14(e). In the system shown Fig. 14(e), a is the radius, θ is the angle made by the line segment $OS(\theta)$ and the x axis, $S(\theta)$ is a monopole source at the angle θ, r is the distance from the origin O to the observation point P, α is the angle made by the line segment OP and the z axis, and R is the distance from the monopole source $S(\theta)$ to P.

A theoretical model of a circular array source is a ring source in combination with a delay system, where the delay pattern is given by $\tau_\theta = a(1+\sin\theta)/c$. When the volume velocity per an unit arc Δs of the ring source is $\dot{Q}e^{j\omega t}$, the velocity potential $\phi(\alpha)$ at the observation point P caused by the ring source is given by

$$\begin{aligned}\phi(\alpha) &= \frac{a\dot{Q}}{4\pi r} e^{j\{\omega t - k(r+a)\}} \int_0^{2\pi} e^{j2ka \sin(\alpha/2)\cos x} dx \\ &= \frac{a\dot{Q}}{2r} e^{j\{\omega t - k(r+a)\}} J_0\left(2ka \sin\frac{\alpha}{2}\right),\end{aligned} \tag{32}$$

where J_0 is the zero-order Bessel function.

The directivity factor is given by

$$D(\alpha) = \left| \frac{\phi(\alpha)}{\phi(0)} \right| = \left| J_0\left(2ka \sin\frac{\alpha}{2}\right) \right|. \tag{33}$$

2. The directivity index classified

From a practical viewpoint for the theoretical sound power level, a surface enclosing the source is a sphere of radius 1 m. The segments of the sphere can be calculated using

$$\Delta S_i = r^2 \int \sin\alpha d\alpha \int d\beta, \tag{34}$$

where $r = 1$ m is the radius of the sphere, α is the directional angle from the z axis ($0 \leqslant \alpha \leqslant \pi$) and β is the directional angle from the orthogonal projection of the x-y plane onto the x axis ($0 \leqslant \beta \leqslant 2\pi$).

Therefore, the dimensions of each model are (a) a dipole source ($d = 0.5$ m), (b) a model sound source with two point sources ($d = 0.5$ m), (c) a model sound source with six point sources ($d = 0.1$ m), (d) a line source ($d = 0.5$ m), (e) a circular diaphragm ($a = 0.5$ m), (f) an end fired line source ($d = 0.5$ m), and (g) a circular array source with delay units ($a = 0.5$ m). For the dipole source, the power of each monopole source is set to 1 W. For the other models, the sound intensity level is set to IL = 120 dB at $\alpha = 0°$.

a. Relationship between the directivity index and the decibel expression for the maximum directivity ratio ($D_r > 1/2$). There is no angle at which the fall-off in sound intensity from the axial direction is as great as 3 dB (D_r

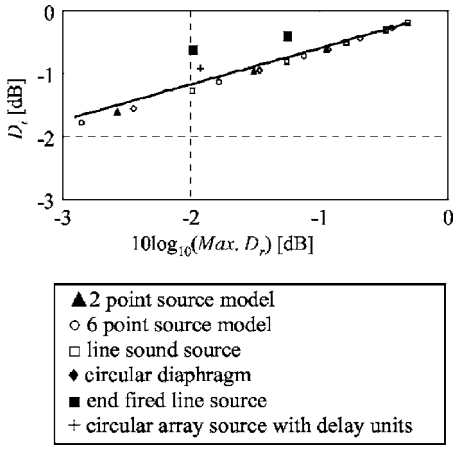

FIG. 15. Relationship between the directivity index D_i and the decibel expression for the maximum directivity ratio ($D_r > 1/2$).

$>1/2$). Figure 15 shows the relationship between the directivity index D_i and the decibel expression for the maximum directivity ratio ($D_r > 1/2$). From this figure, the relationship between the directivity index and the decibel expression for the maximum directivity ratio ($D_r > 1/2$) is analyzed by fitting coefficients in the following log model through simple regression analysis:

$$D_i = 0.574 \times 10 \log(\text{Max } D_r) - 0.021, \tag{35}$$

where the correlation coefficient is 0.9247.

b. Relationship between the directivity index and the beamwidth ($D_r \leqslant 1/2$). The beamwidth is measured as the angle in degrees between the 3 dB half power points. Figure 16 shows the relationship between the directivity index D_i and the beamwidth ($D_r \leqslant 1/2$). From this figure, the relationship between the directivity index D_i and the beamwidth ($D_r \leqslant 1/2$) is analyzed by fitting coefficients in the following natural log (ln) model through simple regression analysis:

$$D_i = 7.243 \ln(\text{Beamwidth}) - 32.279, \tag{36}$$

where the correlation coefficient is 0.9305.

Here, for a dipole source, the error in the sound power level when $r=1$ m relative to the theoretical value of the sound power level calculated from Eq. (23) is less than 0.01 dB.

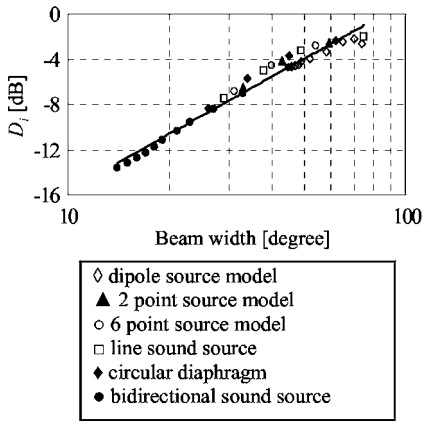

FIG. 16. Relationship between the directivity index D_i and the beamwidth ($D_r \leqslant 1/2$).

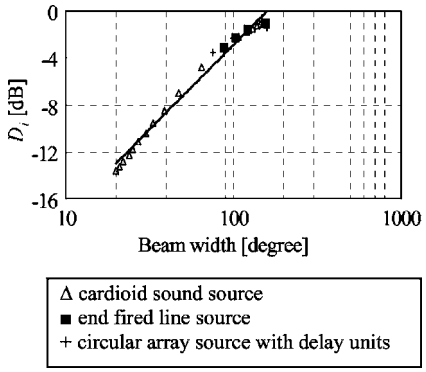

FIG. 17. Relationship between the directivity index D_i and the beamwidth of the cardioid pattern.

c. Relationship between the directivity index and the beamwidth for the cardioid pattern. Figure 17 shows the relationship between the directivity index D_i and the beamwidth for the cardioid pattern. From this figure, the relationship between the directivity index D_i and the beamwidth for the cardioid pattern is analyzed by fitting coefficients in the following ln model through simple regression analysis:

$$D_i = 6.250 \ln(\text{Beamwidth}) - 31.679, \tag{37}$$

where the correlation coefficient is 0.9384.

d. Relationship between the partial directivity index ΔD_i *and the beamwidth of major lobes.* The directivity factor becomes more pronounced at higher frequencies, and minor lobes develop in addition to major lobes. The radiation of sound is zero at certain angles from the axial direction of the source, and also has local maximi. The minor lobes are usually much weaker than the major lobe. Therefore, we only consider the major lobes here, and define the partial sound power for the major lobe. The sharpness of the major lobe is determined by the beamwidth. Figure 18 shows the relationship between the partial directivity index ΔD_i and the beamwidth of major lobes.

From this figure, the relationship between the partial di-

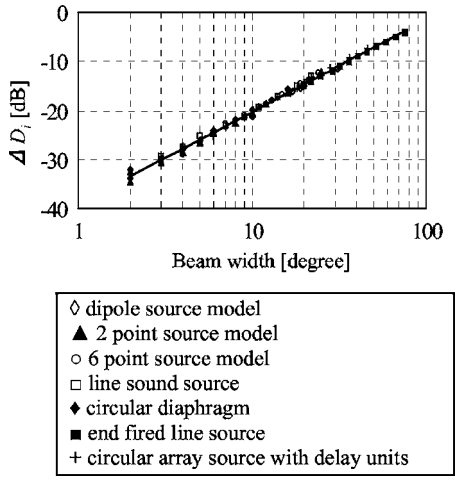

FIG. 18. Relationship between the partial directivity index ΔD_i and the beamwidth of the major lobes.

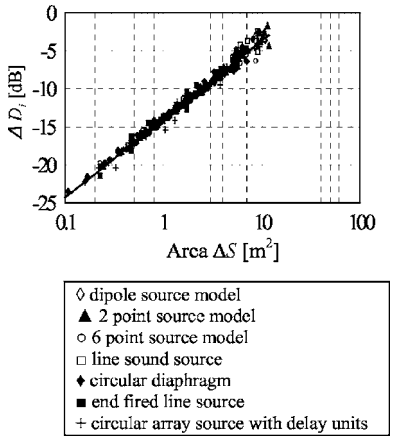

FIG. 19. Relationship between the partial directivity index ΔD_i and the surface area of the minor lobes.

rectivity index ΔD_i and the beamwidth of the major lobes is analyzed by fitting coefficients in the following ln model through simple regression analysis:

$$\Delta D_i = 8.190 \ln(\text{Beamwidth}) - 39.147, \tag{38}$$

where the correlation coefficient is 0.8812.

e. Relationship between the partial directivity index ΔD_i *and the surface area of the minor lobes.* In general, the larger the extent of the radiator, the sharper the major lobe and the greater the number of minor lobes will be. The partial sound power of the minor lobes is determined by the peak sound intensity level and the partial directivity index ΔD_i. The partial directivity index ΔD_i of the minor lobes is correlated with each surface area. The radiation of sound has a dip in the sound intensity level at a certain angle α_1 from the axial direction of the source. The next dip in sound intensity level is at α_2. Therefore, the surface area ΔS of minor lobes can be calculated with Eq. (34) integrated from α_1 to α_2, i.e., the partial sound power of only one minor lobe is considered. Since the surface enclosing the source is a sphere, the influence on the partial sound power of minor lobes by the surface area is large.

Figure 19 shows the relationship between the partial directivity index ΔD_i and the surface area of the minor lobes. From this figure, the relationship between the partial directivity index ΔD_i and the surface area of minor lobes is analyzed by fitting coefficients in the following ln model through simple regression analysis:

$$\Delta D_i = 4.487 \ln(\text{Area}) - 13.981, \tag{39}$$

where the correlation coefficient is 0.8874.

Having completed the measurements, the sound power is determined by summing the partial powers for the major lobe and the minor lobes, that is, if $\text{IL}_{\text{peak}n}$ is the intensity in W/m^2 of the nth measurement ($n=1$: IL_{peak} of the major lobe and $n \geqslant 2$: IL_{peak} of the minor lobes), and ΔD_{in} is the partial directivity index predicted from the beamwidth of the major lobe [$n=1$; Eq. (38)] and from the surface area of the minor lobes [$n \geqslant 2$; Eq. (39)], then:

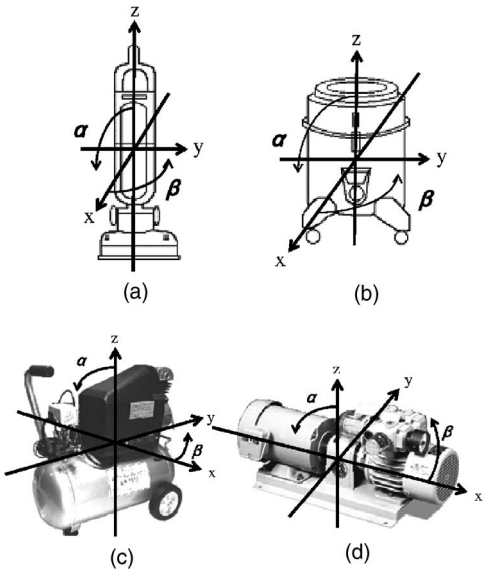

FIG. 20. Spherical coordinates in a three-dimensional system: $0 \leqslant \alpha \leqslant \pi$, and $0 \leqslant \beta < 2\pi$. (a) Broom type vacuum cleaner, (b) industrial vacuum cleaner, (c) air compressor, and (d) dry pump.

$$\text{PWL\_}D_i = \sum_{n=1}^{N} (\text{IL}_{\text{peak}n} + 10 \log_{10} 4\pi + \Delta D_{in}), \tag{40}$$

where N is the number of peaks.

B. Experiment

Practically all sound radiators have pronounced directional effects. This is particularly true when the source is radiating sound waves at high frequencies.

The following discusses experimentally whether sound power can be measured from the ln models of the preceding section.

1. Measurement procedure

The following four machines were selected

(a) A broom type vacuum cleaner (National MC-u30p, $W \times D \times H = 0.3 \times 0.28 \times 0.6$ m^3, electric power consumption: 430 W, number of fans: 6, a single-phase series ac commutator motor), as shown in Fig. 20(a). A rotational frequency of 3033 rpm was used.

(b) An industrial vacuum cleaner (National MC-G250, $W \times D \times H = 0.3 \times 0.3 \times 0.4$ m^3, electric power consumption: 1050 W, number of fans: 6, a single-phase series ac commutator motor), as shown in Fig. 20(b). A rotational frequency of 1910 rpm was used.

(c) An air compressor (TRUSCO ER-1525, $W \times D \times H = 0.55 \times 0.33 \times 0.6$ m^3, electric power consumption: 1200 W), as shown in Fig. 20(c). A discharge rate of 106 l/min was used.

(d) A dry pump[27] (ORION KRX3-SS-4002-G1, $W \times D \times H = 0.5 \times 0.27 \times 0.27$ m^3, electric power consumption: 400 W), as shown in Fig. 20(d). A rotational frequency of 1730 rpm, a discharge pressure of 40 kPa, a throughput of 280 l/min, and a flow rate of 685 l/min were used.

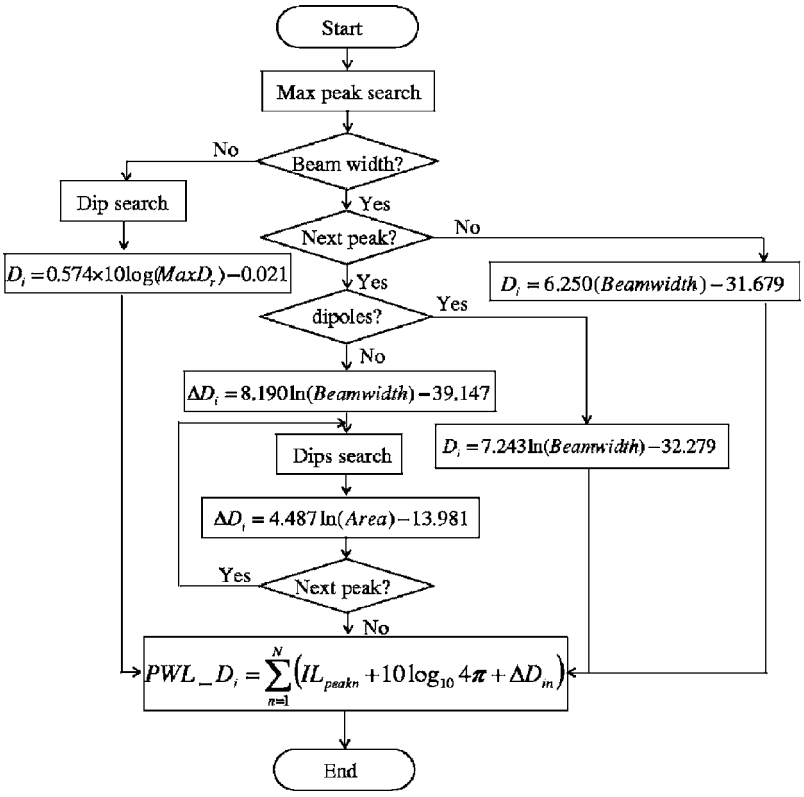

FIG. 21. Flowchart of the proposed measurement procedure.

The objective is to arrive at the total sound intensity passing through the measurement surface. The experiment was done in an anechoic room (Shinshu University; 60 m^3). Our three-dimensional sound intensity probe was set up in a hemisphere of radius 1 m with a handmade turntable. Each product was rotated by the turntable (0.04°/pulse) with a pulse motor and pulse motor control system (see Fig. 10). Figure 20 shows the three-dimensional spherical coordinates, where α is the angle from the positive z axis ($0 \leqslant \alpha \leqslant \pi$) and β is the angle from the x axis in the x-y plane ($0 \leqslant \beta < 2\pi$). To determine the sound power (PWL_D_i) of each machine, the procedure shown in the flowchart in Fig. 21 was used. The procedure is as follows.

(a) Find the local maximum peak sound intensity level as a function of frequency from 200 Hz to 2 kHz.
(b) Check whether the directivity has symmetry. Determine the beamwidth. If there is no beamwidth, the directivity index is found using Eq. (35) from the decibel expression for the maximum directivity ratio ($D_r > 1/2$).
(c) Determine whether there is a beamwidth and no other sound intensity peak. The directivity index is found using Eq. (37) from the beamwidth of the cardioid pattern.
(d) Determine whether there is another sound intensity peak and beamwidth. The directivity index is found using Eq. (36) from the beamwidth ($D_r \leqslant 1/2$).
(e) Determine whether there is another sound intensity peak, i.e., minor lobe. The partial directivity index for the major lobe is found using Eq. (38) from the maximum sound intensity peak and the beamwidth.
(f) Find the second sound intensity peak, i.e., minor lobe, and the side dips which are used to calculate the surface area (m^2). The partial directivity index for the minor lobe is found using Eq. (39) from the surface area ΔS calculated with Eq. (34) integrated from α_1 to α_2.
(g) Repeat (e) and (f) until the desired result has been achieved. Finally, calculate the sound power using Eq. (40).

The sound power level based on ISO 9614-1[8] was measured for comparison. For this standard sound power determination, the intensity passing through the measurement surface was integrated by measuring at a sufficient number of points on the surface. In an anechoic room (Research Institute of Nagano Pref.; 215.6 m^3), the intensity probe microphone (B&K 3545, 1/2 in. microphones, gap: 12 mm, bias error[12] from 200 Hz to 5 kHz: 0.2 dB) was set up on a robot arm (NITTOBO MT-3000 TYPE2). A dual channel real-time analyzer (B&K 2133A) was used for sound power determination. The number of measurement points required to satisfy Eqs. (15) and (16) were: 96 for the two kinds of vacuum cleaners,[28] 110 for the air compressor, and 63 for the dry pump.

2. Results and discussion

Table I shows the level differences (engineering grade) from 200 Hz to 2 kHz between ISO 9614-1[8] (PWL: 96 points) and the sound power determined from the proposed minimum measurement data for the broom type vacuum cleaner. From Table I, it can be found that the minimum number of measurement points is from 2 to 8 for engineering grade sound power determination. For the industrial vacuum cleaner, the minimum number of measurement points is 2 from 200 Hz to 1.25 kHz as shown in Table II. However, the number of points is 8 at 1.6 kHz, and because the number of

TABLE I. Level difference (engineering grade) between ISO 9614-1 (PWL: 96 points) and the sound power determined from the proposed minimum measurement data for a broom type vacuum cleaner.

Frequency (Hz)	200	250	315	400	500	630	800	1000	1250	1600	2000
PWL: 96 points (dB)	52.8	53.3	54.9	59.6	62.8	61.4	63.3	67.4	70.1	69.3	68.0
PWL_D_i (dB)	51.3	52.2	53.0	59.9	61.1	60.5	61.9	66.6	70.3	70.3	67.8
Difference (dB)	1.46	1.18	1.86	0.28	1.70	0.90	1.42	0.75	0.22	1.03	0.14
Number of data	5	8	2	2	2	8	2	2	2	2	2
IL_{peak1} (dB)	44.8	46.3	47.4	52.7	55.7	54.8	56.7	61.8	66.3	64.7	60.1
Beamwidth (°)	14	31	67	86	65	29	63	59	52	67	94
D_i *or* ΔD_i (dB)	−17.5	−11.0	−5.40	−3.84	−5.59	−11.6	−5.78	−6.19	−6.98	−5.40	−3.28
ln model	Eq. (38)	Eq. (38)	Eq. (37)	Eq. (37)	Eq. (37)	Eq. (38)	Eq. (37)	Eq. (37)	Eq. (37)	Eq. (37)	Eq. (37)
IL_{peak2} (dB)	43.4	43.2				51.5					
ΔS (m^2)	10.9	8.44				10.6					
D_i *or* ΔD_i (dB)	−3.26	−4.38				−3.39					
IL_{peak3} (dB)		42.5				48.9					
ΔS (m^2)		2.92				0.98					
D_i *or* ΔD_i (dB)		−9.20				−14.0					
ln model	Eq. (39)	Eq. (39)				Eq. (39)					

TABLE II. Level difference (engineering grade) between ISO 9614-1 (PWL: 96 points) and the sound power determined from the proposed minimum measurement data for an industrial vacuum cleaner.

Frequency (Hz)	200	250	315	400	500	630	800	1000	1250	1600	2000
PWL: 96 points (dB)	54.1	57.3	61.0	57.2	58.1	63.2	64.7	61.9	58.1	59.4	61.2
PWL_D_i (dB)	53.4	57.0	61.6	57.9	59.4	63.4	65.6	61.1	59.0	59.7	62.5
Difference (dB)	0.72	0.32	0.64	0.67	1.23	0.22	0.93	0.82	0.88	0.33	1.33
Number of data	2	2	2	2	2	2	2	2	2	8	17
IL_{peak1} (dB)	47.2	50.1	56.0	51.0	52.5	58.0	59.0	57.6	51.5	53.0	56.0
Beamwidth (°)	74	82	67	82	82	65	79	48	91	29	20
D_i *or* ΔD_i (dB)	−4.78	−4.14	−5.40	−4.14	−4.14	−5.59	−4.37	−7.48	−3.48	−11.6	−14.6
ln model	Eq. (37)	Eq. (37)	Eq. (37)	Eq. (37)	Eq. (37)	Eq. (37)	Eq. (37)	Eq. (37)	Eq. (37)	Eq. (38)	Eq. (38)
IL_{peak2} (dB)										52.0	55.5
ΔS (m^2)										6.92	3.55
D_i *or* ΔD_i (dB)										−5.31	−8.30
IL_{peak3} (dB)										52.0	55.5
ΔS (m^2)										2.13	0.48
D_i *or* ΔD_i (dB)										−10.7	−17.3
IL_{peak4} (dB)											55.0
ΔS (m^2)											2.71
D_i *or* ΔD_i (dB)											−9.51
IL_{peak5} (dB)											53.0
ΔS (m^2)											2.36
D_i *or* ΔD_i (dB)											−10.1
IL_{peak6} (dB)											52.5
ΔS (m^2)											1.84
D_i *or* ΔD_i (dB)											−11.3
ln model										Eq. (39)	Eq. (39)

TABLE III. Level difference (engineering grade) between ISO 9614-1 (PWL: 110 points) and the sound power determined from the proposed minimum measurement data for an air compressor.

Frequency (Hz)	200	250	315	400	500	630	800	1000	1250	1600	2000
PWL: 110 points (dB)	71.6	75.8	83.3	80.5	73.6	72.2	69.2	65.5	65.2	65.6	70.6
PWL_D_i (dB)	72.6	75.4	84.5	80.6	74.7	71.4	69.0	65.8	65.8	66.3	71.1
Difference (dB)	0.98	0.40	1.22	0.15	1.02	0.84	0.20	0.28	0.55	0.65	0.56
Number of data	2	2	2	2	2	2	2	2	2	2	2
IL_{peak1} (dB)	69.5	73.0	80.1	74.8	68.4	67.6	65.3	63.4	62.6	62.5	67.4
Beamwidth (°)	45	40	55	70	75	50	50	40	45	50	50
D_i (dB)	−7.89	−8.62	−6.63	−5.12	−4.69	−7.23	−7.23	−8.62	−7.89	−7.23	−7.23
ln model	Eq. (37)	Eq. (37)	Eq. (37)	Eq. (37)	Eq. (37)	Eq. (37)	Eq. (37)	Eq. (37)	Eq. (37)	Eq. (37)	Eq. (37)

minor lobes is 5 at 2 kHz, the number of points increases to 17. For the air compressor, the minimum number of measurement points is 2 from 200 Hz to 2 kHz as shown in Table III. For the dry pump, the minimum number of measurement points is from 2 to 5 as shown in Table IV.

From the results, it can be seen that sound power determination based on the proposed minimum measurement data yields an accuracy in the low-frequency range (200–630 Hz) of under 1.99 dB, and an accuracy in the midfrequency range (800 Hz to 2 kHz) of under 1.49 dB.

Consequently, it can be said that the proposed searching techniques are effective for sound power determination based on minimum measurement data.

IV. CONCLUSIONS

Because sound intensity measurements offer several ways to locate and identify parts of devices and machines radiating the most acoustic energy, first, a full vector intensity probe with a rotating and variable directional microphone system was developed for canceling both phase mismatch and position errors.

(a) The probe has three pairs of microphones at an equal spacing of 30 mm that are set up on the x, y, and z axes and share the same observation point.
(b) The symmetrical arrangement of the proposed system with six microphones is effective to calibrate both the intrinsic phase mismatch and the position errors by rotating four microphones on the y-z plane.
(c) Variation of the directional separation angle is effective for source location using the null search method on the y-z plane.
(d) The system can identify the maximum sound intensity level and beamwidth of the major lobe, and the peak sound intensity levels of minor lobes.

Second, a procedure for sound power determination based on minimum measurement data was proposed. Results show the following.

(e) The sound power level and directivity of the sound source can be used to calculate the maximum sound intensity level of the major lobe, the distance r from the sound source to the measuring point, the directivity index, and the peak sound intensity levels of the minor lobes.
(f) The directivity indices can be obtained from five curves: (1) the relationship between the directivity index and the decibel expression for the maximum directivity ratio ($D_r > 1/2$), (2) the relationship between the directivity index and the beamwidth ($D_r \leqslant 1/2$), (3) the relationship between D_i and the beamwidth of the cardioid pattern, (4) the relationship between the partial D_i and the beamwidth of major lobes, and (5) the relationship between the partial D_i and the surface area of the minor lobes.

TABLE IV. Level difference (engineering grade) between ISO 9614-1 (PWL: 63 points) and the sound power determined from the proposed minimum measurement data for a dry pump.

Frequency (Hz)	200	250	315	400	500	630	800	1000	1250	1600	2000
PWL: 63 points (dB)	71.0	79.9	74.7	70.9	69.4	70.7	70.4	71.6	70.6	64.2	64.3
PWL_D_i (dB)	69.2	80.6	72.7	69.4	70.6	69.9	68.9	72.3	71.2	63.9	63.1
Difference (dB)	1.88	0.70	1.99	1.57	1.28	0.77	1.49	0.66	0.57	0.30	1.20
Number of data	2	2	5	5	2	2	5	2	2	2	2
IL_{peak1} (dB)	66.8	76.8	73.1	66.1	65.2	64.5	67.0	66.6	62.8	58.0	59.3
Beamwidth [°]	40	50	20	30	40	40	30	70	60	70	50
D_i *or* ΔD_i (dB)	−8.62	−7.23	−14.6	−11.3	−5.56	−5.56	−11.3	−5.12	−2.62	−5.12	−7.23
ln model	Eq. (37)	Eq. (37)	Eq. (38)	Eq. (38)	Eq. (36)	Eq. (36)	Eq. (38)	Eq. (37)	Eq. (36)	Eq. (37)	Eq. (37)
IL_{peak2} (dB)			65.4	62.9			62.6				
ΔS (m^2)			5.16	4.71			3.14				
D_i *or* ΔD_i (dB)			−6.58	−7.04			−8.85				
ln model			Eq. (39)	Eq. (39)			Eq. (39)				

(g) From 200 Hz to 2 kHz each level difference (engineering grade) between ISO 9614-1 (PWL: 96 points) and the sound power determined from the proposed minimum measurement data of four practical sound sources yields an accuracy in the low-frequency range (200–630 Hz) of under 1.99 dB, and an accuracy in the mid-frequency range (800 Hz to 2 kHz) of under 1.49 dB.
(h) The minimum number of measurement points is from 2 to 17 for engineering grade sound power determination.

Consequently, it can be said that the proposed intensity measurement system is effective for sound power determination based on minimum measurement data.

[1]T. J. Schultz, "Acoustic wattmeter," J. Acoust. Soc. Am. **28**, 693–699 (1956).
[2]F. J. Fahy, "Measurement of acoustics intensity using the cross-spectral density of two microphone signals," J. Acoust. Soc. Am. **62**, 1057–1059 (1977).
[3]M. P. Waser and M. J. Crocker, "Introduction to the two-microphones cross-spectral method of determining sound intensity," Noise Control Eng. J. **22**, 76–85 (1984).
[4]G. Pavic, "Measurement of sound intensity," J. Sound Vib. **51**, 533–545 (1977).
[5]P. S. Watkinson, "The practical assessment of errors in sound intensity measurement," J. Sound Vib. **105**, 255–263 (1986).
[6]E. Frederiksen and O. Schultz, "Pressure microphones for intensity measurements with significantly improved phase properties," Brüel & Kjaer Tech. Rev. **4**, 11–23 (1986).
[7]G. Hübner, "Sound intensity measurement method–Errors in determining the sound power levels of machines and its correlation with sound field indicators," in *Proceedings of Inter-Noise*, 1987, pp. 1227–1230.
[8]ISO 9614-1, *Acoustics–Determination of Sound Power Levels of Noise Sources Using Sound Intensity–Part 1: Measurement at Discrete Points*. (ISO, Geneva, Switzerland, 1990).
[9]J. Y. Chung, "Cross-spectral method of measuring acoustic intensity without error caused by instrument phase mismatch," J. Acoust. Soc. Am. **64**, 1613–1616 (1978).
[10]G. Krishnappa, "Cross-spectral method of measuring acoustic intensity by correcting phase and gain mismatch errors by microphone calibration," J. Acoust. Soc. Am. **69**, 307–310 (1981).
[11]F. Jacobsen, "A simple and effective correction for phase mismatch in intensity probes," Appl. Acoust. **33**, 165–180 (1991).
[12]T. Yanagisawa and N. Koike, "Cancellation of both phase mismatch and position errors with rotating microphones in sound intensity measurements," J. Sound Vib. **113**, 117–126 (1987).
[13]N. Koike and T. Yanagisawa, "Separation of sound intensity vector using variable directional microphone," *Proceedings of Inter-Noise 1994*, pp. 1761–1764.
[14]ISO 9614-2, "Acoustics - determination of sound power levels of noise sources using sound intensity - part 2: Measurement by scanning, (ISO, Geneva, Switzerland, 1996).
[15]F. J. Fahy, *Sound Intensity* (Elsevier Applied Science, London, 1989), Secs. 6.3.1, 6.9.2, 6.9.4, and 8.2.
[16]F. J. Fahy, in Ref. 15, Sec. 6.2.2.
[17]J. K. Thompson and D. R. Tree, "Finite difference approximation errors in acoustic intensity measurements," J. Sound Vib. **75**, 229–238 (1981).
[18]T. Wada, K. Furihata, T. Yanagisawa, and N. Koike, "Measurement of vector sound intensity of moving vehicles for automatic supervision," *Proceedings of Inter-Noise* 2002, p. N375.
[19]F. J. Fahy, in Ref. 15, Sec. 5.2.2.
[20]F. J. Fahy, in Ref. 15, Sec. 9.2.
[21]H. F. Olson, *Acoustical Engineering* (Van Nostrand, Princeton, 1957), Chaps. 2–6, pp. 30–211.
[22]L. L. Beranek, *Acoustics* (McGraw-Hill, New York, 1954), Chaps. 4–6, pp. 91–182.
[23]L. E. Kinsler and A. R. Frey, *Fundamentals of Acoustics* (Wiley, New York, 1950), Chap. 7, pp. 162–197.
[24]P. M. Morse, *Vibration and Sound*, 2nd ed. (McGraw-Hill, New York, 1948), Chap. 7, pp. 294–380.
[25]M. Kawamura, *Introduction to Electro-acoustic Engineering*, 25th ed. (Shokodo, Tokyo, 1995), Chap. 3, pp. 39–53.
[26]T. Hayasaka and S. Yoshikawa, *Theory of Sound and Vibration* (Maruzen, Tokyo, 1974), Chap. 18, pp. 569–602.
[27]T. Shimada, T. Yanagisawa, and K. Tagawa, "Characterization of noise generated by a dry pump by using a vane vacuum pump and noise reduction methods," Noise Control Eng. J. **35**, 95–101 (1990).
[28]S. Nagata, K. Furihata, and T. Yanagisawa, "Relation between close curved surface and measurement points of sound power levels for electric cleaners using sound intensity method," *Proceedings of Inter-Noise* 2000, pp. 3793–3797.